

A PET Tracer for Brain α_{2C} Adrenoceptors, ^{11}C -ORM-13070: Radiosynthesis and Preclinical Evaluation in Rats and Knockout Mice

Eveliina Arponen¹, Semi Helin¹, Päivi Marjamäki², Tove Grönroos², Patrik Holm³, Eliisa Löyttyniemi⁴, Kjell Någren¹, Mika Scheinin⁵, Merja Haaparanta-Solin², Jukka Sallinen³, and Olof Solin^{1,6}

¹Radiopharmaceutical Chemistry Laboratory, Turku PET Centre, University of Turku, Turku, Finland; ²MediCity/PET Preclinical Laboratory, Turku PET Centre, University of Turku, Turku, Finland; ³Orion Pharma, Research and Development, Turku, Finland;

⁴Department of Biostatistics, University of Turku, Turku, Finland; ⁵Department of Pharmacology, Drug Development and Therapeutics, University of Turku, and Unit of Clinical Pharmacology, Turku University Hospital, Turku, Finland; and ⁶Accelerator Laboratory, Åbo Akademi University, Turku, Finland

We report the development of a PET tracer for α_{2C} adrenoceptor imaging and its preliminary preclinical evaluation. α_{2C} adrenoceptors in the human brain may be involved in various neuropsychiatric disorders, such as depression, schizophrenia, and neurodegenerative diseases. PET tracers are needed for imaging of this receptor system in vivo. **Methods:** High-specific-activity ^{11}C -ORM-13070 (1-[(S)-1-(2,3-dihydrobenzo[1,4]dioxin-2-yl)methyl]-4-(3- ^{11}C -methoxymethylpyridin-2-yl)-piperazine) was synthesized by ^{11}C -methylation of O-desmethyl-ORM-13070 with ^{11}C -methyl triflate, which was prepared from cyclotron-produced ^{11}C -methane via ^{11}C -methyl iodide. Rats and mice were investigated in vivo with PET and ex vivo with autoradiography. The specificity of ^{11}C -ORM-13070 binding to α_2 adrenoceptors was demonstrated in rats pretreated with atipamezole, an α_2 adrenoceptor antagonist. The α_{2C} adrenoceptor selectivity of the tracer was determined by comparing tracer binding in wild-type and α_{2A} - and α_{2AC} adrenoceptor knockout (KO) mice. ^{11}C -ORM-13070 and its radioactive metabolites in rat plasma and brain tissue were analyzed with radio-high-performance liquid chromatography and mass spectroscopy. Human radiation dose estimates were extrapolated from rat biodistribution data. **Results:** The radiochemical yield, calculated from initial cyclotron-produced ^{11}C -methane, was $9.6\% \pm 2.7\%$ (decay-corrected to end of bombardment). The specific activity of the product was $640 \pm 390 \text{ GBq}/\mu\text{mol}$ (decay-corrected to end of synthesis). The radiochemical purity exceeded 99% in all syntheses. The highest levels of tracer binding were observed in the striatum and olfactory tubercle of rats and control and α_{2A} KO mice—that is, in the brain regions known to contain the highest densities of α_{2C} adrenoceptors. In rats pretreated with atipamezole and in α_{2AC} KO mice, ^{11}C tracer binding in the striatum and olfactory tubercle was low, similar to that of the frontal cortex and thalamus, regions with low densities of α_{2C} adrenoceptors. Two radioactive metabolites were found in rat plasma, but only one of them was found in the brain; their identity was not revealed. The estimated effective radiation dose was comparable with the average exposure level in PET studies with ^{11}C tracers. **Conclusion:** An efficient method for the

radiosynthesis of ^{11}C -ORM-13070 was developed. ^{11}C -ORM-13070 emerged as a potential novel radiotracer for in vivo imaging of brain α_{2C} adrenoceptors.

Key Words: α_{2C} adrenoceptor; radiosynthesis; ^{11}C -ORM-13070; autoradiography; PET

J Nucl Med 2014; 55:1171–1177

DOI: 10.2967/jnumed.113.135574

The α_2 adrenoceptor subtypes α_{2A} , α_{2B} , and α_{2C} mediate many of the physiologic effects of noradrenaline and adrenaline. The α_{2C} adrenoceptor subtype is a potential drug target for the treatment of neuropsychiatric disorders, such as depression, schizophrenia, and dementia (1,2).

In the rodent brain, the highest densities of α_{2C} adrenoceptors are found in the striatum and olfactory tubercle (3,4). The striatum also contains the highest density of α_{2C} adrenoceptors in post-mortem human brain (5).

Several radioligands have been evaluated for PET imaging of brain α_2 adrenoceptors, such as ^{11}C -MK-912 (6), [*O*-methyl- ^{11}C] RS-15385-197 (7), ^{11}C -mirtazapine (8), ^{11}C -R107474 (9), and ^{11}C -yohimbine (10), but they do not differentiate between the α_2 adrenoceptor subtypes. Two recently developed PET tracer candidates, ^{11}C -MBF and ^{11}C -JP-1302, are selective for the α_{2C} adrenoceptor subtype, but they do not readily enter the brain (11).

In this study, a novel PET tracer for α_{2C} adrenoceptor imaging was developed and evaluated in rats and in wild-type (WT) and α_{2A} and α_{2AC} adrenoceptor knockout (KO) mice. We report here the radiosynthesis of ^{11}C -ORM-13070 (1-[(S)-1-(2,3-dihydrobenzo[1,4]dioxin-2-yl)methyl]-4-(3- ^{11}C -methoxymethylpyridin-2-yl)-piperazine) with high specific activity (SA). The receptor specificity of ^{11}C -ORM-13070 binding was assessed ex vivo in rats using pretreatment with atipamezole (Antisedan; Orion Pharma), a subtype-nonspecific antagonist of α_2 adrenoceptors. Selectivity for the α_{2C} adrenoceptor subtype was demonstrated by the use of WT control mice and mice devoid of α_{2A} adrenoceptors and mice lacking both α_{2A} and α_{2C} adrenoceptors (α_{2A} KO and α_{2AC} KO mice).

Received Dec. 17, 2013; revision accepted Mar. 17, 2014.
For correspondence or reprints contact: Olof Solin, Turku PET Centre, Kiinamyllynkatu 4-8, FI-20520 Turku, Finland.
E-mail: olof.solin@abo.fi
Published online May 5, 2014.
COPYRIGHT © 2014 by the Society of Nuclear Medicine and Molecular Imaging, Inc.

The fraction of unmetabolized ^{11}C -ORM-13070 was determined in samples of rat plasma and brain using radiochromatography. The biodistribution of radioactivity after ^{11}C -ORM-13070 injection was investigated in the brain and peripheral organs of rats in vivo with PET/CT and ex vivo using both autoradiography and radioactivity counting. A radiation dose for humans was extrapolated from rat biodistribution data.

MATERIALS AND METHODS

Production of ^{11}C -Methane

^{11}C was prepared by the $^{14}\text{N}(\text{p},\alpha)^{11}\text{C}$ nuclear reaction using 17-MeV protons, which were produced with an MGC-20 cyclotron (Efremov Institute), and was obtained as ^{11}C -methane. The target gas was nitrogen, containing 5% hydrogen (AGA).

Radiosynthesis of ^{11}C -ORM-13070

The desmethyl precursor (2-{4-[(S)-1-(2,3-dihydrobenzo[1,4]dioxin-2-yl)methyl]piperazin-1-yl}-pyridin-3-yl)-methanol (ORM-13333), the reference compound (ORM-13070), and atipamezole were provided by Orion Pharma. All other reagents were purchased from commercial suppliers and were used without further purification.

^{11}C -ORM-13070 (**2**) was synthesized by ^{11}C -methylation of its precursor, *O*-desmethyl ORM-13070 (ORM-13333) (**1**), with ^{11}C -methyl triflate (Fig. 1), which was prepared from cyclotron-produced ^{11}C -methane via ^{11}C -methyl iodide. ^{11}C -methyl iodide was synthesized from ^{11}C -methane and iodine in a gas phase reaction at 720°C (12). ^{11}C -methyl triflate was prepared online from ^{11}C -methyl iodide by passing ^{11}C -methyl iodide through a silver triflate/graphitized carbon column, using argon gas as a carrier at 200°C (13).

The desmethyl precursor (1.0 mg, 3.0 μmol) was dissolved in acetonitrile (200 μL) in a 1-mL reaction vial sealed with a septum and a screw-cap (Reacti-Vial; Pierce). Freshly prepared tetrabutyl ammonium hydroxide (3.0 μL , 1.0 M) was added to the reaction solution. The ^{11}C -methyl triflate was transferred to the solution (at 0°C) in a stream of argon gas (15 mL/min). The reaction mixture was heated in an 80°C oil bath for 3 min. ^{11}C -ORM-13070 was purified by high-performance liquid chromatography (HPLC) on a semipreparative size column, using the system described in the supplemental data (supplemental materials are available at <http://jnm.snmjournals.org>). After removal of the mobile phase by vacuum rotary evaporation, the ^{11}C -ORM-13070 batches used for preclinical experiments were formulated in propylene glycol/ethanol/0.1 M phosphate buffer (10/5/85, v/v/v; volume, 3.5 mL) and passed through a sterile Acrodisc Syringe Filter with HT Tuffryn Membrane (0.2 μm , 25 mm; Pall Corp.) into the sterile end-product vial for injection. The analytic HPLC system is described in the supplemental data.

Animals

Male Sprague–Dawley (originally from Harlan), locally outbred rats ($n = 34$), weighing 292 ± 31 g, and male α_{2A} KO ($n = 6$), α_{2AC} KO ($n = 5$), and C57Black WT mice ($n = 6$), weighing 33 ± 3 g, were used in this study. α_{2A} KO and α_{2AC} KO mice were orig-

inally a gift from Dr. Brian K. Kobilka, Stanford University (14) and were bred locally; WT control mice were obtained from the Jackson Laboratory. The animals were housed at the Central Animal Laboratory of the University of Turku under standard conditions (temperature, 21°C ; humidity, $55\% \pm 5\%$; lights on from 6:00 AM to 6:00 PM), with free access to standard food and tap water. Animal care complied with the guidelines of the International Council of Laboratory Animal Science. This study was approved by the Animal Experiment Board of the Province of Southern Finland.

In Vivo PET Imaging

PET imaging was performed using an Inveon Multimodality PET/CT scanner (Siemens Medical Solutions) designed for small laboratory animals. Isoflurane, 2% or 2.5%, in oxygen was used to anesthetize the rats or mice, respectively, for 30 min before radiotracer injection. The animals were kept warm with a heating pad and a bubble-wrap cover, and their eyes were protected with ophthalmic gel. CT transmission scans were obtained to correct for attenuation. Dynamic emission scans were acquired for 60 min in 3-dimensional list mode, with an energy window of 350–650 keV. Scans were started immediately after the intravenous bolus injection of ^{11}C -ORM-13070. The injected dose for rats ($n = 4$) was 48 ± 13 MBq, and the injected mass was 0.2 ± 0.1 nmol/kg (range, 0.1–0.3 nmol/kg). The injected dose for mice ($n = 6$) was 10.7 ± 1.6 MBq, and the injected mass was 6.8 ± 15.1 nmol/kg (range, 0.4–37.7 nmol/kg), as calculated from the SA at the time of injection.

List-mode data were stored into 3-dimensional sinograms, which were then Fourier-rebinned into 2-dimensional sinograms (51 frames; 30×10 , 15×60 , 4×300 , and 2×600 s). Images were reconstructed using 2-dimensional filtered backprojection with a 0.5-mm ramp filter.

To analyze the PET images, volumes of interest were drawn on the striatum and cerebellar cortex with Inveon Research Workplace Image Analysis software (Siemens Medical Solutions). CT images were used as anatomic reference. From the volumes of interest, time–radioactivity curves were obtained for the striatum and cerebellar cortex. Striatum-to–cerebellar cortex radioactivity ratios were then calculated at 5–15 min after injection.

Ex Vivo Autoradiography

Ex vivo autoradiography imaging of brain cryosections was performed at 10 min ($n = 6$) and 30 min ($n = 10$) after injection of ^{11}C -ORM-13070 in rats and at 1 time point (10 min after injection; $n = 11$) in mice. The injected dose for rats was 60 ± 17 MBq, and the injected mass was 2.7 ± 2.0 nmol/kg (range, 0.3–6.9 nmol/kg). The injected dose for mice was 7.4 ± 2.3 MBq, and the injected mass was 6.2 ± 12.4 nmol/kg (range, 0.5–31.4 nmol/kg), as calculated from the SA at the time of injection.

Brains were dissected, weighed, measured for ^{11}C radioactivity, and immediately frozen with isopentane, which was chilled with dry ice. Coronal cryosections (40 μm) were prepared on microscope slides, air dried, and apposed to an imaging plate (Imaging Plate BAS-TR2025; Fuji Photo Film Co.) for approximately 1 h. The imaging plates were scanned with a Fuji BAS-5000 Analyzer.

Digital autoradiographic images were analyzed for count densities (photostimulated luminescence per unit area, PSL/ mm^2) using the Aida 2.14 program (Raytest Isotopenmessgeräte GmbH). Regions of interest were drawn over the frontal cortex, olfactory tubercle, striatum, thalamus, and cerebellar cortex (15). At least 5 sections were analyzed for each brain region of each animal, and background count densities were subtracted from the region-of-interest counts. For each animal, the uptake

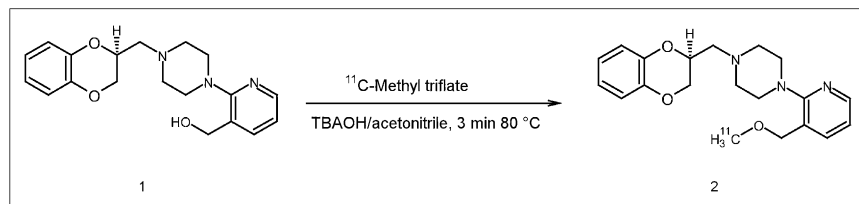


FIGURE 1. Synthesis scheme for ^{11}C -ORM-13070 (**2**) from its precursor ORM-13333 (**1**). TBAOH = tetrabutyl ammonium hydroxide.

of ^{11}C -ORM-13070-derived radioactivity in the brain was evaluated as PSL/mm². Region-to-cerebellar cortex radioactivity ratios were calculated. The cerebellar cortex was used as a reference tissue because of its known low, negligible density of α_{2C} adrenoceptors (4).

The pharmacologic specificity of ^{11}C -ORM-13070 binding in rats was estimated from the decrease in binding after the subcutaneous administration of a dose of atipamezole (1 mg/kg), a subtype-non-selective antagonist of α_2 adrenoceptors. Atipamezole was dissolved in a 0.9% NaCl solution and administered to the rats 40 min before ^{11}C -ORM-13070. The rats were sacrificed 30 min after the tracer injection. The regional distribution of ^{11}C radioactivity in the brains of these rats ($n = 2$) was determined using autoradiography, as described earlier.

Metabolite Analysis and Plasma Protein Binding

^{11}C -ORM-13070 and its radioactive metabolites were analyzed in rat plasma, striatum, and cerebellar cortex using radio-HPLC with a semipreparative C18 column (supplemental data).

Attempts were also made at the Drug Metabolism Laboratory of Orion Pharma to identify the 2 radioactive metabolites formed from ^{11}C -ORM-13070 (supplemental data).

Plasma proteins were precipitated with acetonitrile. The brain samples were homogenized in HPLC mobile phase, deproteinized with acetonitrile, and centrifuged. The supernatants were then injected into the HPLC system for analysis. Chromatograms were manually integrated, and the results were decay-corrected. The fractions of unmetabolized ^{11}C -ORM-13070 and its radioactive metabolites of the total radioactivity present in the samples were analyzed using D-7000 HSM (HPLC System Manager) software (version 3.0; Merck-Hitachi). The protein binding of ^{11}C radioactivity in plasma was determined by ultrafiltration (Microsep 30 kD; Pall Life Sciences). The fraction of protein-unbound radioactivity was expressed as the percentage of the total ^{11}C radioactivity in plasma.

Biodistribution of ^{11}C -ORM-13070 in Rats

^{11}C -ORM-13070 was injected into the tail vein of rats ($n = 15$) under light isoflurane/oxygen anesthesia. The injected radioactivity was 38 ± 7 MBq, and the injected mass was 3.9 ± 5.6 nmol/kg (range, 0.6–15.6 nmol/kg), as calculated from the SA at the time of injection. Rats were sacrificed by CO₂ inhalation at 2 min ($n = 3$), 5 min ($n = 3$), 10 min ($n = 3$), 20 min ($n = 3$), or 40 min ($n = 3$) after the injection of ^{11}C -ORM-13070. Organs and tissues were immediately dissected, weighed, and measured for ^{11}C radioactivity in a 2480 Wizard Gamma Counter (Wallac) or in a well counter (7.62×7.62 cm NaI (TI) crystal; Bicon Inc.).

Dosimetry

Dose estimates for healthy human males (73 kg) were extrapolated from the rat biodistribution data, using the program OLINDA/EX 1.0 (16). On the basis of these extrapolated ^{11}C radioactivity uptake values in human organs, the software was used to calculate the estimated effective organ doses ($\mu\text{Sv/MBq}$).

Statistics

Descriptive statistics are presented by arithmetic means and SDs. Differences in region-to-cerebellar cortex uptake ratios between groups of mice (WT, α_{2A} KO, α_{2AC} KO) were tested separately for each brain region (striatum, olfactory tubercle, frontal cortex, thalamus), using 1-way ANOVA. In addition, pairwise comparisons of the groups against α_{2AC} KO mice were performed with the Dunnett method. All tests were performed 2-sided, with a significance level set at 0.05. The analyses were performed using the SAS System (version 9.3 for Windows [Microsoft]; SAS Institute Inc.).

RESULTS

Synthesis of ^{11}C -ORM-13070

^{11}C -ORM-13070 (**2**) was synthesized by ^{11}C -methylation of the desmethyl precursor (**1**) with ^{11}C -methyl triflate (Fig. 1). The initial radioactivity of ^{11}C -methane was approximately 37 GBq as determined by calibrated Geiger-Müller tubes in the synthesis apparatus, and the average synthesis time was 32 ± 3 min, including the synthesis of ^{11}C -methyl triflate, methylation, HPLC purification, and formulation. The retention times of the precursor and ^{11}C -ORM-13070 in HPLC purification were 3.9 and 7.2 min, respectively.

The radiochemical yield, calculated from the initial ^{11}C -methane (decay-corrected to end of bombardment), was $9.6\% \pm 2.7\%$, and the radioactivity of ^{11}C -ORM-13070 was $1,210 \pm 360$ MBq at end of synthesis. Measured by analytic HPLC, the SA was 640 ± 390 GBq/ μmol (end of synthesis). The chemical purity of the final product, that is, the absence of unknown signals in the ultraviolet trace, was verified by analytic HPLC. The concentration of precursor in the final product was low, at 0.15 nmol/mL or less. The retention times of the precursor and ^{11}C -ORM-13070 in analytic HPLC were 1.4 and 3.6 min, respectively.

The radiochemical purity of the product exceeded 99% in all syntheses ($n = 118$). The final product was radiochemically stable for up to 1 h, as verified by HPLC. Of the synthesized batches, 22 were used for preclinical evaluation.

In Vivo PET/CT

PET/CT imaging of the rat brain showed that the ^{11}C radioactivity uptake in the striatum reached a maximum of 1.8 percentage injected dose per gram (%ID/g) in 1 min after injection. Thereafter, the striatal ^{11}C radioactivity rapidly decreased to a level of about 0.2 %ID/g at 30 min. In the cerebellar cortex, the uptake and clearance of radioactivity were faster than in the striatum. The striatum-to-cerebellar cortex radioactivity ratio reached a maximum of 1.8 in about 10 min after injection, after which the ratio slowly declined to 1.4 at 30 min (Fig. 2).

PET/CT imaging of mice showed that the ^{11}C radioactivity uptake in the brain was similar for WT and α_{2A} KO mice and reached a maximum of 7.8–8.1 %ID/g in about 1 min and decreased to a level of 1.2 %ID/g at 30 min. The striatum-to-cerebellar cortex radioactivity ratios at 5–15 min for α_{2A} KO ($n = 2$),

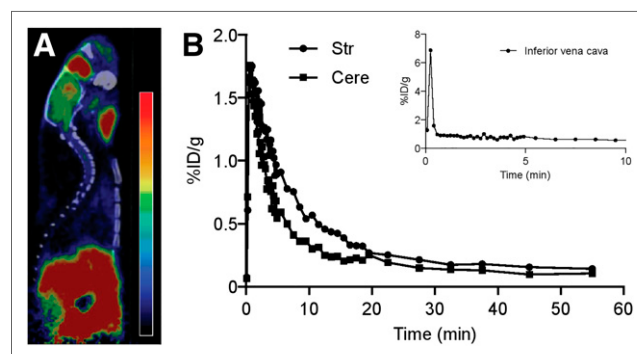


FIGURE 2. (A) Summed maximum-intensity-projection PET/CT image shows ^{11}C radioactivity biodistribution in Sprague-Dawley rat in vivo, for period 5–15 min after tracer injection. (B) Time-radioactivity curves obtained from inferior vena cava, striatum, and cerebellar cortex show rapid clearance of ^{11}C -ORM-13070 from blood and rapid entry into brain. Cere = cerebellar cortex; Str = striatum.

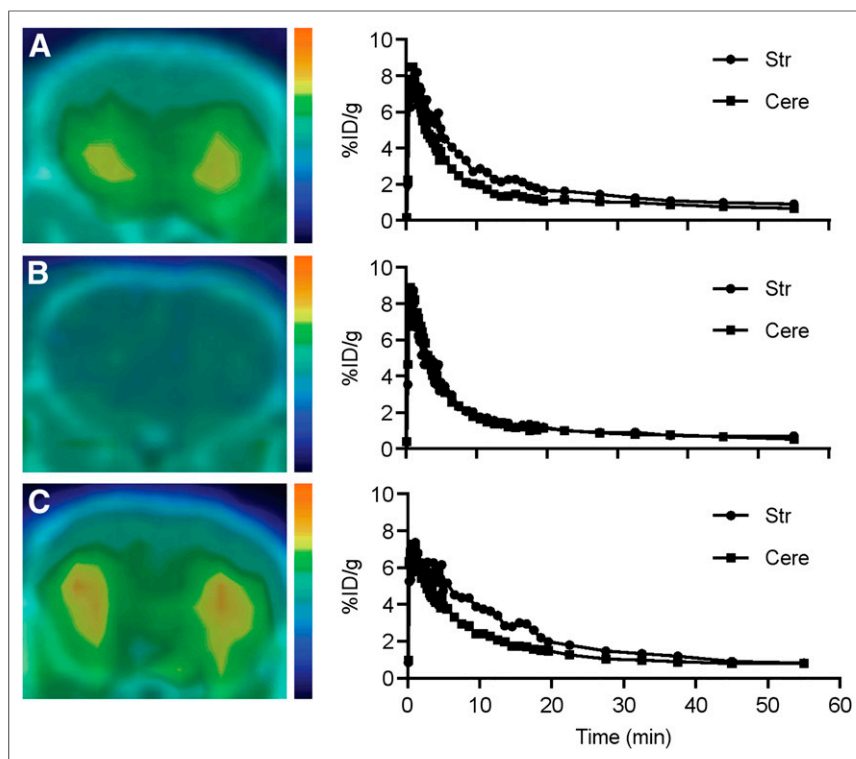


FIGURE 3. Representative ^{11}C -ORM-13070 PET/CT images and time-activity curves for striatum and cerebellar cortex of α_{2A} KO (A), α_{2AC} KO (B), and WT mice (C). α_{2A} KO and WT mice show higher uptake in striatum than cerebellar cortex. No differences in regional uptake were seen in α_{2AC} KO mice. Cere = cerebellar cortex; Str = striatum.

α_{2AC} KO ($n = 2$), and WT mice ($n = 2$) were 1.51–1.51, 1.06–1.09, and 1.51–1.57, respectively. In α_{2AC} KO mice, the uptake in the striatum did not differ from the uptake in the cerebellar cortex (Fig. 3).

Ex Vivo Autoradiography and Specificity of ^{11}C -ORM-13070 Binding

The highest region-to-cerebellar cortex radioactivity ratios in both rats and WT and α_{2A} KO mice were observed in the striatum and olfactory tubercle (Figs. 4 and 5; Supplemental Figs. 1 and 2). In rats pretreated with atipamezole, the ^{11}C radioactivity ratios of the striatum and olfactory tubercle were similar to those of the frontal cortex and thalamus at 30 min after injection—that is, close to 1.0 (Fig. 4). The region-to-cerebellar cortex radioactivity ratios were clearly higher in the striatum and olfactory tubercle in α_{2A} KO and WT mice than α_{2AC} KO mice ($P = 0.024$ and 0.032 for α_{2A} KO vs. α_{2AC} KO, and $P = 0.036$ and 0.091 for WT vs. α_{2AC} KO). α_{2A} KO mice also tended to have higher frontal cortex-to-cerebellar cortex radioactivity ratios than α_{2AC} KO mice ($P = 0.061$) (Fig. 5).

Radioactive Metabolites of ^{11}C -ORM-13070

Intact ^{11}C -ORM-13070 was detected in rat plasma, striatum, and cerebellar cortex at a retention time of 7.3 min in HPLC. One major radioactive metabolite (M1) was detected in all samples, at a retention time of 2.1 min. Another minor radioactive metabolite (M2) was detected at a retention time of 3.4 min. Chromatograms of samples of rat striatum, cerebellar cortex, and plasma at 10 min after injection are shown in Supplemental Figure 3. At 10 min after injection, $32\% \pm 10\%$ of the total

radioactivity was found as intact ^{11}C -ORM-13070 in plasma (Fig. 6). The fraction of intact ^{11}C -ORM-13070 was $89\% \pm 3\%$ ($n = 5$) in the striatum and $81\% \pm 5\%$ ($n = 3$) in the cerebellar cortex at 10 min after injection. At 30 min after injection, the fractions were $77\% \pm 9\%$ ($n = 3$) and $58\%–67\%$ ($n = 2$), respectively. Only M1 was observed in the brain (Supplemental Fig. 3).

Metabolites corresponding to M1 and M2 could not be detected in plasma or brain samples with mass spectroscopy (supplemental data). It is likely that M1 and M2 represent volatile compounds with low molecular weight, not detectable with the used HPLC–mass spectroscopy approaches.

Binding of ^{11}C -ORM-13070–derived radioactivity to plasma proteins decreased over time. The fraction of unbound ^{11}C radioactivity in plasma at 10 min was $32\%–39\%$ and $48\%–58\%$ at 30 min ($n = 2$ for each time point).

Biodistribution in Rats and Dosimetry

The ^{11}C radioactivity uptake in peripheral organs and tissues after injection of ^{11}C -ORM-13070 in rats is presented in Supplemental Table 1. The uptake of ^{11}C -ORM-13070 into tissues was rapid, reaching its maximum in most tissues at 2 min after injection. The highest initial ^{11}C radioactivity was found in the adrenal glands. High levels of ^{11}C radioactivity were also recorded in the small intestine, kidneys, pancreas, and liver.

Dose estimates for an adult human were extrapolated from the rat biodistribution data. The organs with the highest estimated doses were the small intestine and adrenal glands, with 36.8 and $14.4 \mu\text{Sv/MBq}$, respectively. The estimated effective human radiation dose of ^{11}C -ORM-13070 was $4 \mu\text{Sv/MBq}$.

DISCUSSION

We aimed to develop ^{11}C -ORM-13070 as a PET tracer for brain α_{2C} adrenoceptor imaging and to evaluate its suitability for PET imaging. Several α_2 adrenoceptor PET tracer candidates have been evaluated previously, but they have either lacked receptor subtype selectivity or shown poor penetration into the brain (6–11). Receptor binding assays have been performed with ORM-13070 and recombinant human α_2 adrenoceptor subtypes (17) and more than 100 other potential receptor targets (Cerep Discovery Profile) to determine the receptor profile of the tracer. The calculated binding affinities were as follows (binding affinity values [nM], with corresponding 95% confidence intervals in parentheses): α_{2C} adrenoceptor, 3.8 ($2.0–7.3$); α_{2B} adrenoceptor, 23 ($14–38$); and α_{2A} adrenoceptor, 109 ($86–138$). Screening assays for binding to more than 100 other potential receptors and targets indicated only weak or no activity of ORM-13070 (Orion Pharma, unpublished data, 2006).

We developed an efficient method for the radiosynthesis of ^{11}C -ORM-13070 and demonstrated, through preclinical evaluation, the

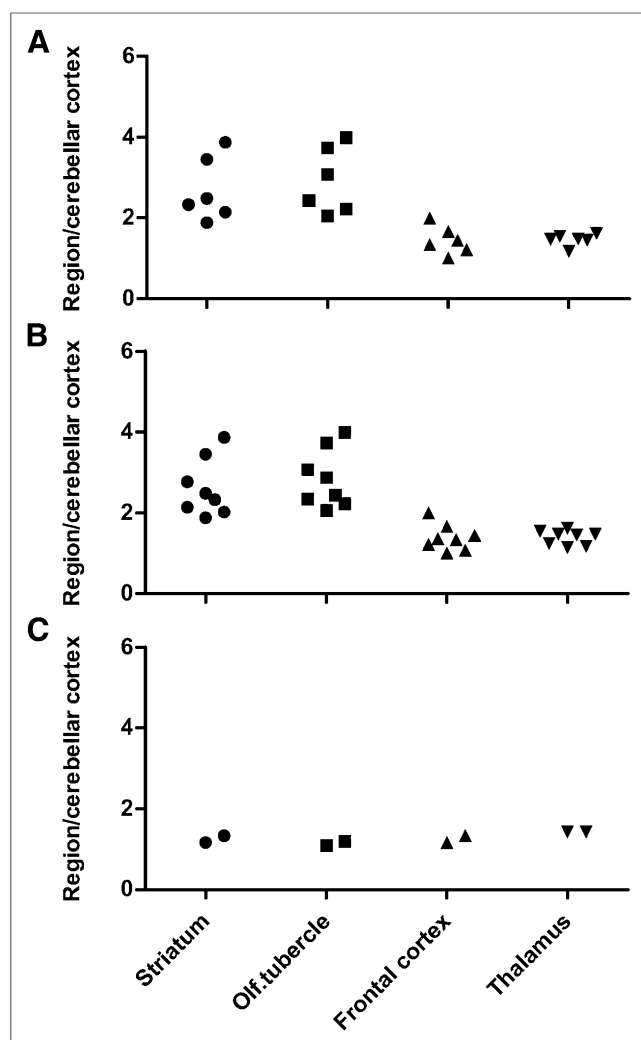


FIGURE 4. Region-to-cerebellar cortex radioactivity ratios for Sprague-Dawley rats were calculated from ex vivo autoradiograms. Brain cryosections were obtained 10 min (A) and 30 min (B) after ^{11}C -ORM-13070 injection without pretreatment and at 30 min after ^{11}C -ORM-13070 injection with atipamezole pretreatment (C) (mean \pm SD, $n = 2$ –8). Olf. = olfactory.

specificity and selectivity of the tracer for α_{2C} adrenoceptors in rats and mice and its suitability for in vivo imaging. Of the brain regions investigated here, α_{2C} adrenoceptor expression has been shown to be most abundant in the striatum and olfactory tubercle, less abundant in the frontal cortex, and very low in the thalamus and cerebellum (4). In general, our results with ^{11}C -ORM-13070 agree with these previous findings.

High SA is important for imaging of brain receptors that are expressed at low density, to avoid significant receptor occupancy, subsequent errors in the quantitation of binding sites, and possible pharmacologic effects. The high SA of ^{11}C -ORM-13070 was achieved using in-target-produced ^{11}C -methane with high SA as starting material for ^{11}C -methyl iodide production (18) and subsequent synthesis of ^{11}C -ORM-13070. ^{11}C -ORM-13070 was synthesized with good radiochemical yield, and the radiochemical purity exceeded 99% in all syntheses.

Initial in vivo PET imaging and ex vivo autoradiographic studies of the rat brain after ^{11}C -ORM-13070 injection

showed that the distribution of tracer uptake was consistent with the known expression pattern of α_{2C} adrenoceptors in the brain (Figs. 2, 3C, and 4; Supplemental Figs. 1 and 2) (4,5,14). The specificity of ^{11}C -ORM-13070 binding to α_{2} adrenoceptors was demonstrated by pretreating rats with the subtype-nonselective α_{2} adrenoceptor antagonist atipamezole. This pretreatment completely blocked the binding of ^{11}C -ORM-13070 in the striatum and olfactory tubercle (Fig. 4; Supplemental Fig. 1).

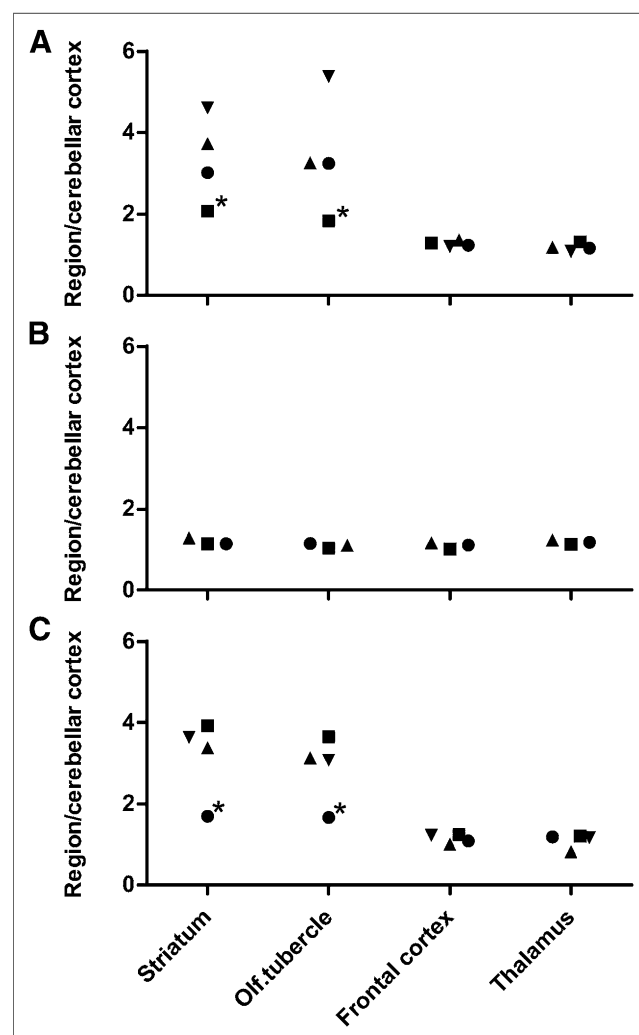


FIGURE 5. Region-to-cerebellar cortex radioactivity ratios for α_{2A} KO (A), α_{2AC} KO (B), and C57Black WT (C) mice were calculated from ex vivo autoradiograms of 40- μm brain cryosections, which were obtained 10 min after ^{11}C -ORM-13070 injection. Each animal is marked with individual marker (■, ●, ▲, and ▼). Region-to-cerebellar cortex radioactivity ratios were higher in striatum and olfactory tubercle of α_{2A} KO and WT mice than α_{2AC} KO mice ($P = 0.024$ and 0.032 for α_{2A} KO vs. α_{2AC} KO, and $P = 0.036$ and 0.091 for WT vs. α_{2AC} KO). Trend toward significance was also observed for difference between α_{2A} KO and α_{2AC} KO mice for frontal cortex-to-cerebellar cortex radioactivity ratio ($P = 0.061$). Asterisks (*) denote individual animals dosed with ^{11}C -ORM-13070 with relatively low SA (injected mass, 31.0 and 31.4 nmol/kg), highlighting importance of high SA in imaging of receptors with low abundance and high affinity. Olf. = olfactory.

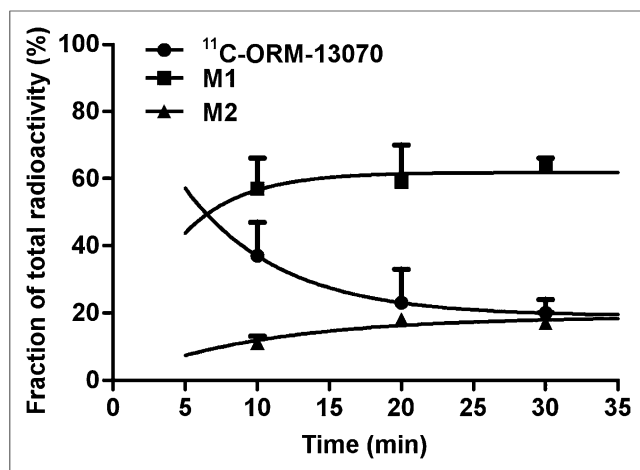


FIGURE 6. In vivo metabolism of ^{11}C -ORM-13070 in blood plasma of Sprague-Dawley rats. Time-radioactivity curves obtained from high-performance liquid chromatograms of plasma samples at 10, 20, and 30 min after injection of ^{11}C -ORM-13070 are shown. ^{11}C -ORM-13070 was metabolized into 2 polar radiolabeled metabolites, and fractions of unmetabolized tracer and radiolabeled metabolites changed over time.

α_2 adrenoceptor subtype selectivity of the tracer was demonstrated by comparison of tracer uptake in the brains of α_{2A} KO, α_{2AC} KO, and WT control mice (Figs. 3 and 5; Supplemental Fig. 2). The ^{11}C -ORM-13070 binding in the brains of α_{2A} KO and WT mice was similar. There was little tracer binding in the brains of α_{2AC} KO mice. These results demonstrated the α_{2C} adrenoceptor selectivity of the tracer.

Time-activity curves of specific tracer uptake into the striatum and cerebellum of rats and mice (Figs. 2 and 3) showed fast uptake into and clearance from the brain, which are suitable qualities for a tracer used for imaging of brain α_{2C} adrenoceptors. Moreover, radio-HPLC of striatal and cerebellar cortex tissue homogenates showed that the intact tracer was the most abundant radioactive species present. Thus, the radioactivity signal in the rat brain was mainly derived from intact ^{11}C -ORM-13070 (Supplemental Fig. 3).

The amount of ^{11}C radioactivity increased over time in the gastrointestinal tract, indicating that the ^{11}C radioactivity from ^{11}C -ORM-13070 was mainly cleared via this route (Supplemental Table 1; Fig. 2). High initial ^{11}C radioactivity uptake was found in the adrenal glands, lungs, and heart (Supplemental Table 1). Radio-HPLC of plasma as a function of time showed relatively rapid metabolism of the parent compound, where the fraction of intact tracer was approximately 20% of total ^{11}C radioactivity at 30 min after injection. Two polar radioactive metabolites (M1 and M2) were observed in plasma (Fig. 6), but only one of these was observed in brain samples (Supplemental Fig. 3).

Metabolites corresponding to M1 and M2 could not be identified in plasma or brain samples with extensive mass spectroscopy analysis (supplemental data). The plasma protein binding of the radioactivity decreased over time, and the unbound fraction at 30 min (48%–58%) corresponded with the amount of M1 shown in Figure 6. The major radioactive metabolite M1 is likely to be a small volatile compound with no affinity for the target receptor, but its possible impact on human brain PET studies still calls for further clarification.

On the basis of the effective dose estimates derived from rats in this study, a 500-MBq injection of ^{11}C -ORM-13070 to a 73-kg human would result in a radiation dose of 2 mSv. This is in line with the average expected exposure in PET studies of brain receptors with other ^{11}C tracers (19).

α_{2C} adrenoceptors are present in brain regions involved in the processing of sensory information and in the control of motor- and emotion-related activities (4). They may be involved in various neurodegenerative and neuropsychiatric disorders. The anatomic distribution of α_{2C} adrenoceptors in the brain appears to be well conserved between rodents and humans (4,5). Therefore, results from studies on α_{2C} adrenoceptors in rodent models are likely to be relevant for α_{2C} adrenoceptor physiology and pharmacology in the human brain.

The α_{2C} adrenoceptor is a potential drug target for the treatment of neurodegenerative and neuropsychiatric diseases. A PET tracer for α_{2C} adrenoceptors is expected to be useful for preclinical and clinical drug development (20). The tracer has been introduced to human use (21,22), as evidenced by 4 already completed clinical PET trials with ^{11}C -ORM-13070 (ClinicalTrials.gov identifiers NCT00735774, NCT00829907, NCT01435213, and NCT01794975).

CONCLUSION

An efficient method for the radiosynthesis of ^{11}C -ORM-13070 with high SA was developed. In vivo PET imaging showed high uptake of ^{11}C -ORM-13070 in the striatum of rats and mice. ^{11}C -ORM-13070 emerged as a selective tracer for imaging of α_{2C} adrenoceptors in vivo in mice and rats and is, therefore, a promising PET tracer for imaging of α_{2C} adrenoceptors in humans.

DISCLOSURE

The costs of publication of this article were defrayed in part by the payment of page charges. Therefore, and solely to indicate this fact, this article is hereby marked "advertisement" in accordance with 18 USC section 1734. This work was supported by grants from Orion Pharma, EU IMI-JU NEWMEDS grant 115008, and the Academy of Finland (project 266891). No other potential conflict of interest relevant to this article was reported.

REFERENCES

1. Scheinin M, Sallinen J, Haapalinna A. Evaluation of the α_{2C} -adrenoceptor as a neuropsychiatric drug target: studies in transgenic mouse models. *Life Sci*. 2001;68:2277–2285.
2. Sallinen J, Höglund I, Engström M, et al. Pharmacological characterization and CNS effects of a novel highly selective α_{2C} -adrenoceptor antagonist JP-1302. *Br J Pharmacol*. 2007;150:391–402.
3. Scheinin M, Lomasney JW, Hayden-Hixson DM, et al. Distribution of α_2 -adrenergic receptor subtype gene expression in rat brain. *Brain Res Mol Brain Res*. 1994;21:133–149.
4. Holmberg M, Fagerholm V, Scheinin M. Regional distribution of α_{2C} -adrenoceptors in brain and spinal cord of control mice and transgenic mice overexpressing the α_{2C} -subtype: an autoradiographic study with [^3H]RX821002 and [^3H] rauwolscine. *Neuroscience*. 2003;117:875–898.
5. Fagerholm V, Rokka J, Nyman L, et al. Autographic characterization of α_{2C} -adrenoceptors in the human striatum. *Synapse*. 2008;62:508–515.
6. Shiue C, Pleus R, Shiue G, et al. Synthesis and biological evaluation of ^{11}C -MK-912 as an α_2 -adrenergic receptor radioligand for PET studies. *Nucl Med Biol*. 1998;25:127–133.

7. Hume SP, Hirani E, Opacka-Juffry J, et al. Evaluation of [*O*-methyl-¹¹C]RS-15385-197 as a positron emission tomography radioligand for central α_2 -adrenoceptors. *Eur J Nucl Med*. 2000;27:475–484.
8. Smith DF, Dyve S, Minuzzi L, et al. Inhibition of ¹¹C-mirtazapine binding by α_2 -adrenoceptor antagonist studied by positron emission tomography in living porcine brain. *Synapse*. 2006;59:463–471.
9. Van der Mey M, Windhorst A, Klok R, et al. Synthesis and biodistribution of ¹¹C-R107474, a new radiolabeled α_2 -adrenoceptor antagonist. *Bioorg Med Chem*. 2006;14:4526–4534.
10. Jakobsen S, Pedersen K, Smith D, et al. Detection of α_2 -adrenergic receptors in brain of living pig with ¹¹C-yohimbine. *J Nucl Med*. 2006;47:2008–2015.
11. Kawamura K, Akiyama M, Yui J, et al. In vivo evaluation of limiting brain penetration of probes for α_{2C} -adrenoceptor using small-animal positron emission tomography. *ACS Chem Neurosci*. 2010;1:520–528.
12. Larsen P, Ulin J, Dahlström K, et al. Synthesis of ¹¹C-iodomethane by iodination of ¹¹C-methane. *Appl Radiat Isot*. 1997;48:153–157.
13. Jewett DM. A simple synthesis of ¹¹C-methyl triflate. *Int J Rad Appl Instrum A*. 1992;43:1383–1385.
14. Hein L, Altman JD, Kobilka BK. Two functionally distinct α_2 -adrenergic receptors regulate sympathetic neurotransmission. *Nature*. 1999;402:181–184.
15. Paxinos G, Watson C. *The Rat Brain in Stereotaxic Coordinates*. San Diego, CA: Academic Press; 1986:53–99.
16. Stabin MG, Sparks RB, Crowe E. OLINDA/EXM: the second-generation personal computer software for internal dose assessment in nuclear medicine. *J Nucl Med*. 2005;46:1023–1027.
17. Ruuskanen JO, Laurila J, Xhaard H, et al. Conserved structural, pharmacological and functional properties among the three human and five zebrafish α_2 -adrenoceptors. *Br J Pharmacol*. 2005;144:165–177.
18. Henriksen G. ¹¹C-Labelled tracers for use in PET: concepts and selected labeling strategies for preparative radiosynthesis. In: Wester HJ, ed. *Pharmaceutical Radiochemistry (I)*. Fürstfeldbruck, Germany: SCINTOMICS; 2010:75–102.
19. van der Aart J, Hallett WA, Rabiner EA, et al. Radiation dose estimates for carbon-11-labelled PET tracers. *Nucl Med Biol*. 2012;39:305–314.
20. Finnema S, Varnas K, Stepanov V, et al. Amphetamine decreases binding of the novel α_{2C} -adrenoreceptor radioligand ¹¹C-ORM-13070 in monkey brain. *Neuroimage*. 2010;52(suppl):S61–S62.
21. Luoto P, Suilamo S, Oikonen V, et al. ¹¹C-ORM-13070, a novel PET tracer for brain α_{2C} -adrenoceptors: radiometabolism, plasma pharmacokinetics, whole-body distribution and radiation dosimetry in healthy man. *Eur J Nucl Med Mol Imaging*. 2012;39(suppl 2):S359.
22. Scheinin M, Hirvonen M, Johansson J, et al. Evaluation of ¹¹C-ORM-13070 as a PET tracer for α_{2C} -adrenoceptors in the human brain. In: Eiden L, ed. *Catecholamine Research in the 21st Century: Abstracts and Graphical Abstracts, 10th International Catecholamine Symposium 2012*. Oxford, U.K.: Elsevier; 2013:162.



The Journal of
NUCLEAR MEDICINE

A PET Tracer for Brain $\alpha_2\text{C}$ Adrenoceptors, ^{11}C -ORM-13070: Radiosynthesis and Preclinical Evaluation in Rats and Knockout Mice

Eveliina Arponen, Semi Helin, Päivi Marjamäki, Tove Grönroos, Patrik Holm, Eliisa Löyttyniemi, Kjell Någren, Mika Scheinin, Merja Haaparanta-Solin, Jukka Sallinen and Olof Solin

J Nucl Med. 2014;55:1171-1177.

Published online: May 5, 2014.

Doi: 10.2967/jnumed.113.135574

This article and updated information are available at:

<http://jnm.snmjournals.org/content/55/7/1171>

Information about reproducing figures, tables, or other portions of this article can be found online at:

<http://jnm.snmjournals.org/site/misc/permission.xhtml>

Information about subscriptions to JNM can be found at:

<http://jnm.snmjournals.org/site/subscriptions/online.xhtml>

The Journal of Nuclear Medicine is published monthly.
SNMMI | Society of Nuclear Medicine and Molecular Imaging
1850 Samuel Morse Drive, Reston, VA 20190.
(Print ISSN: 0161-5505, Online ISSN: 2159-662X)

© Copyright 2014 SNMMI; all rights reserved.